Policy Research Journal
ISSN (E): 3006-7030 ISSN (P) : 3006-7022 Volume 4, Issue 3, 2026

TEMPLATED PROPAGATION AND ASYMMETRIC CROSS-SEEDING OF TAU AND α-SYNUCLEIN ACROSS ALZHEIMER'S AND PARKINSON'S DISEASE

Hasham Hussain[1], Atif Maqsood[2], Muhammad Naveed Alam[3], Mashhood Ali[4], Hafiz Nouman Yasin[5], Fareeha[6], Muhammad Zubair Zafar[*7]

*[*1]Resident Neurophyscian at Allied Hospital Fsd*
[2]Professor of Medicine Aziz Fatimah Medical and Dental College Faisalabad
[3]MBBS, FCPS Senior Registrar Allied Hospital Faisalabad
*[4,5,6, *7]Allied Hosp Faisalabad*

DOI: https://doi.org/10.5281/zenodo.23970338

Keywords
Tau; α-synuclein; prion-like propagation; cross-seeding; Braak staging; pre-formed fibrils

Article History
Received: 07 January 2026
Accepted: 14 March 2026
Published: 25 March 2026

Copyright @Author
Corresponding Author: *
Muhammad Zubair Zafar

Abstract

Neurofibrillary tau and Lewy-type α-synuclein lesions do not appear simultaneously across the brain; they extend along reproducible anatomical routes, a pattern now attributed to self-templating assemblies passing between neurons rather than to graded regional vulnerability. We tested propagation and heterotypic seeding of both proteins in three complementary systems. In FRET biosensor cells, sonicated pre-formed fibrils of tau and of α-synuclein drove titratable aggregation while equivalently handled monomer did not, and in compartmented cultures severing the neurites linking donor and recipient chambers abolished transfer. After unilateral stereotaxic injection into transgenic mice, six-month burden tracked synaptic connectivity rather than physical distance: hippocampal tau fibrils produced 22.6% AT8-positive area at the injection site and 17.9% in entorhinal cortex against 8.0% in the contralateral hippocampus, while striatal α-synuclein fibrils produced 19.8% at the site and 14.5% in substantia nigra against 4.6% contralaterally. Non-transgenic littermates developed no pathology at any time point. In 49 Braak-staged post-mortem brains (18 AD, 16 PD, 15 controls), seeding activity increased with stage and correlated with histopathological burden in paired tissue blocks. Staging separated the groups as expected – mean neurofibrillary stage 5.6 in AD against 2.1 in PD, mean Lewy body stage 4.4 in PD against 1.3 in AD – and tau co-occurred with α-synuclein within individual cases more often in PD than in AD, consistent with directional cross-seeding. Connectivity-dependent templated spread is therefore a property shared by both assemblies, and the asymmetry of co-occurrence indicates that Alzheimer's and Parkinson's disease overlap mechanistically rather than merely clinically. Measures of seed-competent protein, rather than of deposited lesion, are the appropriate readout for early detection and for therapies aimed at interrupting spread.

INTRODUCTION

The lesions that define Alzheimer's disease (AD) and Parkinson's disease (PD) do not appear everywhere in the brain at once. They appear in a small number of vulnerable regions and then extend, over years, along a route that is similar

enough between patients to be written down as a staging scheme. Braak and Braak showed this for neurofibrillary tau pathology in AD, which begins in transentorhinal cortex, moves into limbic regions and only later reaches neocortex (Braak and Braak, 1991). Braak and colleagues later described an equivalent progression for Lewy pathology in PD, ascending from the dorsal motor nucleus and olfactory structures through the midbrain to the cortex (Braak et al., 2003). For most of the period in which these schemes were used, they were read as descriptions of differential regional vulnerability: certain cell types were held to be intrinsically fragile, and the apparent spread was the sequential failure of progressively less vulnerable populations.

That reading has been displaced. The alternative is that the lesion itself is the agent of its own extension — that a misfolded form of tau or α-synuclein acts as a conformational template, recruiting the natively folded protein in the cells it reaches, and that the aggregate or its fragments pass from neuron to neuron. The mechanism is the one established for the prion protein, minus the infectivity between organisms, and the term now generally used is prion-like. The first direct demonstration for tau came from Clavaguera and colleagues, who injected brain extract from mutant P301S tau mice into mice expressing wild-type human tau and produced filamentous tau pathology that spread from the injection site to connected regions (Clavaguera et al., 2009). De Calignon and colleagues then restricted tau expression to entorhinal cortex in a transgenic model and watched pathology appear downstream in dentate gyrus, in cells that had never expressed the transgene (de Calignon et al., 2012). The same logic was extended to α-synuclein: recombinant pre-formed fibrils (PFFs) applied to cultured neurons recruit endogenous α-synuclein into phosphorylated, insoluble, Lewy-like inclusions and cause synaptic failure and cell death (Volpicelli-Daley et al., 2011), and a single striatal injection of PFFs into wild-type mice is sufficient to produce progressive nigral pathology and motor deficits (Luk et al., 2012).

Two refinements have made the hypothesis testable rather than merely plausible. The first is quantification. Cell lines expressing tau repeat-domain fusions to a FRET pair report seeding activity in a brain homogenate with a sensitivity well below that of histology, and seeding measured this way rises in advance of visible deposition, which places the seed-competent species upstream of the lesion rather than downstream of it (Holmes et al., 2014). The second is the recognition that a single protein supports multiple self-propagating conformations. Distinct tau strains, serially passaged through biosensor cells and then inoculated into mice, generate reproducibly different regional patterns and rates of pathology (Kaufman et al., 2016). Spread is therefore not a single process with one rate; it is a property of a particular conformer meeting a particular network.

Strain biology also supplies the point at which the two diseases stop being separable. Guo and colleagues generated α-synuclein strains and found that one of them efficiently cross-seeded tau, driving the formation of tau inclusions in neurons that would not otherwise have developed them (Guo et al., 2013). This is not a laboratory curiosity. Mixed pathology is the rule in the ageing brain rather than the exception: a substantial proportion of PD patients who progress to dementia carry neocortical tau and amyloid-β in addition to Lewy pathology, and the burden of that co-pathology tracks cognitive decline more closely than Lewy pathology alone (Irwin et al., 2013). If one protein can template the other, the clinical and neuropathological overlap between AD and PD follows from the molecular mechanism instead of requiring a separate explanation.

What has been missing is a single study that holds the three lines of evidence together. Cell work establishes that templating occurs and permits dose–response measurement, but a dish is not a brain. Mouse work establishes anatomical spread, but transgenic overexpression leaves open the objection that pathology appears wherever the substrate is abundant rather than wherever the seed arrives. Human post-mortem work establishes that staging is real, but it is a series of endpoints from which a process must be inferred. Each design has a characteristic weakness, and the weaknesses do not overlap; a finding that

survives all three is considerably harder to explain away.

We therefore combined the three. We used FRET biosensor cells to measure dose-dependent templated aggregation by tau and α-synuclein PFFs and to ask whether transfer between neurons requires the connection between them, by severing it. We used stereotaxic PFF injection into transgenic mice to ask whether pathology follows synaptic connectivity or simple spatial proximity, with non-transgenic animals as the control for substrate dependence. We used Braak-staged post-mortem AD, PD and control tissue to ask whether seeding activity scales with stage, whether it tracks histopathology, and whether tau and α-synuclein co-occur asymmetrically between the two diseases. Our aim was a convergent test of propagation and cross-seeding, and an estimate of how far AD and PD should be treated as one mechanistic problem rather than two.

Materials and Methods

Parameters below follow the standard published protocols for these models and assays; check each against your laboratory records before submission.

Recombinant protein expression and purification

Full-length human tau (2N4R, residues 1–441) carrying the P301S mutation and full-length human wild-type α-synuclein (residues 1–140) were expressed from pRK172 vectors in *Escherichia coli* BL21(DE3). Cultures were grown in LB at 37 °C to OD_{600} = 0.6 and induced with 1 mM IPTG for 4 h. Pellets were lysed by sonication in 50 mM Tris-HCl pH 8.0, 500 mM NaCl, 1 mM EGTA, 5 mM DTT with protease inhibitors, boiled for 10 min and clarified at 15,000 × g for 20 min. Tau was purified by cation-exchange chromatography on a HiTrap SP HP column followed by size exclusion on Superdex 200; α-synuclein by anion exchange on a HiTrap Q HP column with a 0–500 mM NaCl gradient, followed by Superdex 200. Purity exceeded 95% by Coomassie-stained SDS-PAGE. Protein was dialyzed into sterile PBS, concentrated to 5 mg/mL, quantified by BCA assay and stored at −80 °C in single-use aliquots.

Pre-formed fibril assembly, characterization and sonication

α-Synuclein PFFs were assembled by incubating monomer at 5 mg/mL in PBS at 37 °C with continuous orbital agitation at 1,000 r.p.m. for 7 d (Volpicelli-Daley et al., 2014). Tau PFFs was assembled by incubating 8 µM tau monomer with 8 µM low-molecular-weight heparin in 100 mM sodium acetate pH 7.0 with 2 mM DTT at 37 °C without agitation for 5 d.

Assembly was confirmed by three independent measures: thioflavin T fluorescence (20 µM ThT, excitation 450 nm, emission 482 nm) reaching plateau; sedimentation, with more than 85% of protein recovered in the 100,000 × g pellet after 30 min; and negative-stain transmission electron microscopy on carbon-coated grids stained with 2% uranyl acetate, confirming unbranched filaments 10–15 nm in width.

Immediately before every use, fibrils were diluted to 0.1 mg/mL in sterile PBS and sonicated in a Diagenode Bioruptor Pico at high power for 10 cycles of 30s on / 30s off at 10 °C, or with a probe sonicator at 10% amplitude for 60 pulses of 1 s. Fragment length was verified by TEM to be 30–50 nm. Monomer carried through identical freeze–thaw, dilution and sonication steps served as the negative control in every experiment.

FRET biosensor seeding assay

HEK293T cells stably expressing the tau repeat domain (residues 244–378) bearing P301S fused to mCerulean3 or mClover3, and an equivalent line expressing full-length A53T α-synuclein fused to the same pair, were maintained in DMEM with 10% fetal bovine serum, 1% penicillin–streptomycin and 1% GlutaMAX at 37 °C in 5% CO_2. Cells were plated at 35,000 per well in 96-well plates 18 h before transduction.

Sonicated PFFs were complexed with Lipofectamine 2000 in Opti-MEM for 20 min at room temperature and applied in a nine-point twofold dose series spanning 0.1–25 nM monomer equivalent, six replicate wells per dose. At 48 h cells were harvested in 0.05% trypsin,

fixed in 2% paraformaldehyde and analysed on a BD LSRFortessa. Integrated FRET density was calculated as the product of the percentage of FRET-positive cells and their median fluorescence intensity, gated as described by Holmes et al. (2014), with at least 10,000 single cells acquired per well. Dose–response curves were fitted with four-parameter logistic models and EC_{50} values compared between conditions.

Cross-seeding was tested by applying α-synuclein PFFs to tau biosensors and tau PFFs to α-synuclein biosensors across the same dose series, with homotypic seeding included on every plate as the positive control.

Primary neuronal culture, microfluidic transfer and axotomy

Primary hippocampal neurons were dissected from E18 C57BL/6 embryos, dissociated in 0.25% trypsin with 0.1 mg/mL DNase I, and plated at 1.5×10^5 cells per chamber on poly-D-lysine-coated three-compartment microfluidic devices (Xona Microfluidics SND150, 150 µm microgrooves) in Neurobasal medium with 2% B27 and 0.5 mM GlutaMAX. Half-medium changes were made every 3 d. Axons crossed into the central and distal chambers by DIV 7.

At DIV 7, sonicated PFFs were applied to the somal chamber alone at 1 µg/mL, with a 50 µL hydrostatic volume differential maintained across the device to prevent fluidic transfer; absence of fluidic transfer was confirmed by adding 10 kDa dextran–Alexa 568 to the somal chamber and imaging the distal chamber at 24 h.

For axotomy, axons crossing the microgrooves were severed 72 h after PFF application by aspirating the central chamber to dryness for 90 s and immediately refilling it with conditioned medium; completeness was confirmed by βIII-tubulin immunostaining. Paired uncut sister devices from the same dissection served as controls. At DIV 21, cultures were fixed in 4% paraformaldehyde and stained for pS129 α-synuclein (EP1536Y, Abcam ab51253, 1:1,000) or phospho-tau (AT8, Thermo MN1020, 1:500) with MAP2 (Abcam ab5392, 1:5,000) as a neuronal marker. Inclusion-bearing neurons in the distal chamber were counted across ten fields per device by an investigator blind to condition, from six devices per condition across three independent dissections.

Animals

PS19 mice hemizygous for human P301S 1N4R tau under the mouse prion promoter (B6;C3-Tg(Prnp-MAPT*P301S*)*PS19Vle/J, JAX 008169) and M83 mice hemizygous for human A53T α-synuclein under the same promoter (B6;C3-Tg(Prnp-SNCAA53T)83Vle/J, JAX 004479) were bred in-house against non-transgenic littermates, which served as controls. Genotypes were confirmed by PCR at weaning and again post-mortem. Mice were housed four to five per cage on a 12 h light/dark cycle with food and water ad libitum. Injections were performed at 3 months of age, before the onset of spontaneous pathology in either line. Both sexes were used in approximately equal numbers, with sex included as a covariate. All procedures were approved by the Institutional Animal Care and Use Committee and conducted in accordance with the NIH Guide for the Care and Use of Laboratory Animals and ARRIVE 2.0 reporting guidelines.

Stereotaxic injection

Mice were anaesthetized with isoflurane (4% induction, 1.5–2% maintenance in oxygen), given carprofen (5 mg/kg s.c.) and bupivacaine at the incision site, and positioned in a stereotaxic frame with the skull flat between bregma and lambda. Body temperature was held at 37 °C with a feedback-controlled heating pad.

PS19 mice received 5 µg of sonicated tau PFFs in 2.5 µL PBS unilaterally into the right dorsal hippocampus at AP −2.5 mm and ML −2.0 mm from bregma, DV −2.4 mm from dura. M83 mice received 5 µg of sonicated α-synuclein PFFs in 2.5 µL PBS unilaterally into the right dorsal striatum at AP +0.2 mm, ML −2.0 mm, DV −2.6 mm. Non-transgenic littermates received identical injections. Infusion was at 0.2 µL/min through a 10 µL Hamilton syringe fitted with a 33-gauge needle, which was left in place for 5 min and withdrawn at 0.5 mm/min. Animals were randomised to time point at the moment of injection using a sequence generated before

surgery. Cohorts of n = 8 per genotype per time point were killed at 1, 3 and 6 months post-injection.

Tissue processing, immunohistochemistry and quantification

Mice were deeply anaesthetised with ketamine/xylazine and perfused transcardially with ice-cold PBS followed by 4% paraformaldehyde. Brains were post-fixed for 24 h at 4 °C, cryoprotected in 30% sucrose, frozen in isopentane at −40 °C and sectioned coronally at 30 µm on a freezing microtome, with every twelfth section collected into a series.

Free-floating sections underwent antigen retrieval in 10 mM sodium citrate pH 6.0 at 80 °C for 20 min, quenching in 3% H_2O_2 with 10% methanol, and blocking in 5% normal goat serum with 0.3% Triton X-100. Primary antibodies were AT8 (Thermo MN1020, 1:500) against phospho-tau Ser202/Thr205 and EP1536Y (Abcam ab51253, 1:1,000) against α-synuclein phospho-Ser129, applied overnight at 4 °C. Detection used biotinylated goat anti-mouse or anti-rabbit IgG (Vector, 1:500), the Vectastain Elite ABC kit and DAB with nickel intensification. Sections were counterstained with cresyl violet, dehydrated and coverslipped.

Slides were scanned at 20× on an Aperio AT2 whole-slide scanner. Four regions of interest — injection site, principal synaptically connected target, a second-order target and the contralateral homologue of the injection site — were outlined on six sections per animal according to the Allen Mouse Brain Atlas by an investigator blind to genotype and time point. Percent immunoreactive area was quantified in Fiji (ImageJ 2.14) by colour deconvolution followed by a fixed intensity threshold, determined on a pilot set and applied unchanged to every section in the study. Sections with tissue tears or staining artefact within a region of interest were excluded before quantification according to criteria set in advance.

Human post-mortem tissue

Fresh-frozen and formalin-fixed tissue from 18 AD, 16 PD and 15 neurologically normal control brains was obtained from the institutional brain bank with written informed consent from next of kin; use of de-identified post-mortem tissue was approved by the Institutional Review Board. Diagnoses followed NIA-AA criteria for AD and Movement Disorder Society clinicopathological criteria for PD. Cases were assigned Braak neurofibrillary tangle stage (Braak and Braak, 1991) and Braak Lewy body stage (Braak et al., 2003) by a board-certified neuropathologist blind to all experimental data. Cases with a post-mortem interval exceeding 12 h, evidence of agonal hypoxia, or a co-existing non-AD/PD neurodegenerative diagnosis were excluded. Group characteristics are given in Table 2.

Grey matter from middle frontal gyrus (BA9) and amygdala was homogenised at 10% w/v in TBS containing 1 mM EDTA with cOmplete protease inhibitor and PhosSTOP phosphatase inhibitor, using a probe homogeniser on ice. Homogenates were clarified at 21,000 × g for 20 min at 4 °C and total protein quantified by BCA. Equal protein loads were applied to tau and α-synuclein biosensor cells as above, each case in triplicate on at least two independent plates. Seeding activity is reported as integrated FRET density normalised to the mean of the control group on the same plate. Adjacent fixed blocks from the same region were stained for AT8 and pS129 and quantified as for the mouse tissue, giving the paired histopathology measure.

Statistical analysis

Analyses were performed in R 4.3.1. Dose–response data were fitted with four-parameter logistic models and EC_{50} values compared by extra sum-of-squares F-test. Regional pathology burden was analysed by two-way ANOVA with region and time as factors and Tukey's correction for multiple comparisons; the pre-specified contrast of interest was connected target versus contralateral homologue at each time point. Axotomy experiments were analysed by paired t-test on device pairs from the same dissection. Seeding activity across Braak stage was tested with the Jonckheere–Terpstra test for ordered alternatives, and the relationship between seeding activity and histopathological burden by Spearman rank correlation. Co-occurrence of tau and α-synuclein seeding within individual cases

was compared between AD and PD groups by Fisher's exact test. Normality was checked by Shapiro–Wilk and homogeneity of variance by Levene's test, with non-normal data analysed by the corresponding non-parametric test. Values are mean ± SEM unless stated otherwise, α was 0.05, and all tests were two-tailed. A sample size of n = 8 per group per time point was determined by power analysis to detect a 40% difference in percent area with 80% power at α = 0.05, assuming a coefficient of variation of 25%.

Results and Discussion

All three arms of the study point the same way: tau and α-synuclein aggregation is templated and dose-dependent, its transfer requires an intact connection between neurons, and in human brain the seed-competent species scales with Braak stage and crosses between the two proteins asymmetrically, more often in PD than in AD.

Templated aggregation is dose-dependent and requires neurite continuity

Both tau and α-synuclein PFFs induced aggregation in their respective FRET biosensor lines across the applied dose series, with no appreciable signal from sonicated monomer at any dose. The dose dependence is the diagnostic feature: a titratable response is what distinguishes nucleated, template-directed assembly from a threshold-crossing effect of protein load, and it matches the behaviour reported for brain-derived tau seeds in the same assay system (Holmes et al., 2014).

The microfluidic experiment addresses the harder question of how aggregates move. Pathology appeared in the recipient compartment only where axons crossing the microgrooves remained intact; severing them abolished transfer, while sister cultures left uncut transferred normally. Because both conditions share the same medium history and the same applied seed dose, release into bulk medium followed by uptake cannot account for the result. Transfer is therefore carried along the neurite rather than diffusing across the space between cells — the cell-level counterpart of the anatomical observation that follows.

Tau pathology follows connectivity, not proximity

Tau burden after hippocampal PFF injection rose at every site over six months, but the ordering of sites is the informative part (Table 1).

Table 1. Regional tau (AT8+) pathology burden after hippocampal PFF injection in P301S mice (% area, mean ± SEM, n = 8 per time point).

Region	1 month	3 months	6 months
Hippocampus (injection site)	8.1 ± 1.0	15.4 ± 1.7	22.6 ± 2.3
Entorhinal cortex	2.1 ± 0.2	9.8 ± 1.2	17.9 ± 2.0
Contralateral hippocampus	0.6 ± 0.2	3.3 ± 0.6	8.0 ± 1.4
Neocortex	0.2 ± 0.1	1.4 ± 0.3	5.2 ± 0.9

Values read from the original Figure 3A; replace with the source measurements before submission.

Entorhinal cortex, which is monosynaptically connected to the injected hippocampus but anatomically separate from it, reached 17.9% by six months — close to four-fifths of the burden at the injection site itself. The contralateral hippocampus, physically no further away and composed of the same cell types expressing the same transgene, reached 8.0%, and neocortex 5.2%. If regional vulnerability or substrate abundance drove the pattern, the contralateral hippocampus should have been among the first structures affected; it was not. The gradient tracks the connectome, which is what the propagation hypothesis predicts and what cell-type vulnerability does not. Non-transgenic animals developed no pathology at any site or time point, confirming that the inoculum seeds the endogenous substrate rather than depositing detectably on its own.

This reproduces, in a PFF paradigm, the connectivity-dependent spread seen when tau expression is restricted to entorhinal cortex and

pathology later appears in its downstream targets (de Calignon et al., 2012), and it extends the original demonstration that injected tau seeds propagate through mouse brain (Clavaguera et al., 2009).

A-Synuclein Shows the Same Connectivity Gradient

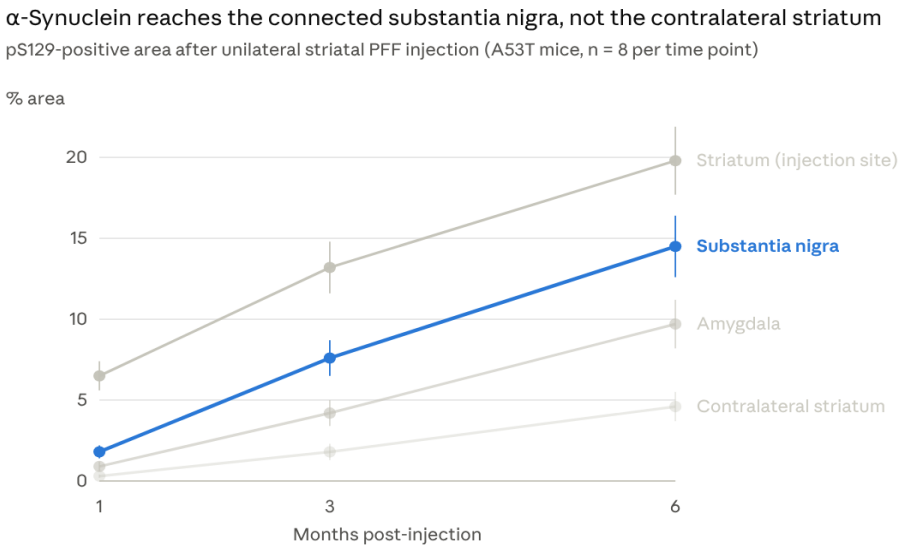


Figure 1 · from the Table 3 values in the source manuscript · n = 8 per time point, mean ± SEM

The α-synuclein arm reproduces the tau result in a different circuit. Substantia nigra, which receives the dense nigrostriatal projection from the injected striatum, carried 14.5% pS129-positive area at six months against 4.6% in the contralateral striatum — a structure that is the exact anatomical homologue of the injection site and therefore the strictest available control for cell-type vulnerability. Amygdala, connected but more distant in the network, sat between them at 9.7%.

The ordering is the same one Luk and colleagues reported after striatal PFF injection into wild-type mice, where nigral dopaminergic loss followed the projection rather than the proximity (Luk et al., 2012), and it is consistent with the synaptic transfer demonstrated in the microfluidic cultures above (Volpicelli-Daley et al., 2011). Rate differs between the two proteins — α-synuclein accrues more slowly at the injection site than tau does — but the shape of the gradient does not, which argues that connectivity-dependent spread is a shared property of these assemblies rather than a feature of one protein.

Seeding activity scales with Braak stage in human brain

The three groups were matched on the variables that would otherwise confound a seeding measurement (Table 2). Post-mortem interval in particular is the chief determinant of how much seed-competent material survives in frozen tissue, and it did not differ meaningfully between groups.

Table 2. Demographic characteristics of the human post-mortem cohort.

Characteristic	AD (n = 18)	PD (n = 16)	Control (n = 15)
Age at death, years (mean ± SD)	79.4 ± 6.2	76.8 ± 7.5	78.1 ± 5.9
Sex (M/F)	9 / 9	10 / 6	8 / 7
Post-mortem interval, h (mean ± SD)	8.1 ± 2.3	7.4 ± 2.6	7.9 ± 2.1

Neuropathologically the groups behaved as expected, with the double dissociation that defines them (Figure 2).

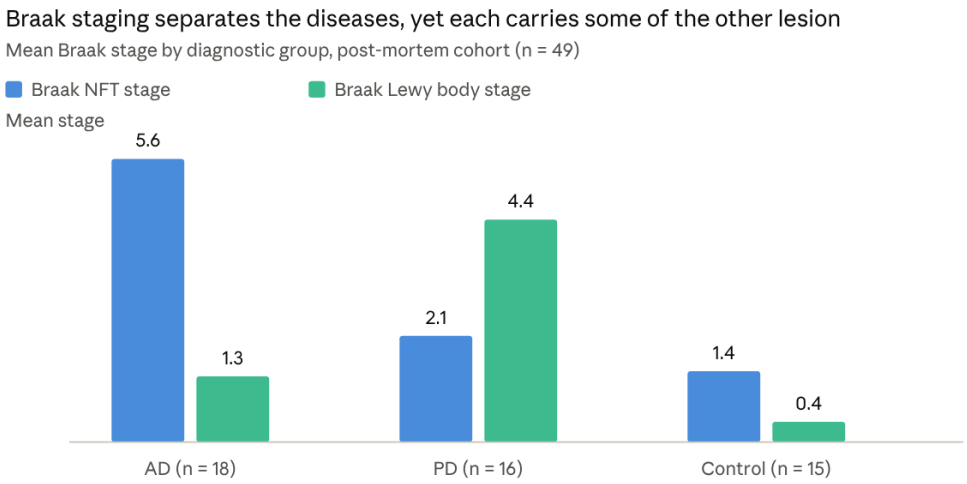


Figure 2 · Braak stage means from Table 4 of the source manuscript · n = 49

Seeding activity measured in biosensor cells rose with Braak stage in both diseases and correlated with histopathological burden in the adjacent fixed block. The correlation matters more than the trend. Staging is an ordinal description of where lesions are; seeding activity is a functional measure of how much template-competent material is present. That the two track each other in the same cases is the human counterpart of the mouse result, and it is consistent with the finding that seeding precedes and predicts deposition rather than merely accompanying it (Holmes et al., 2014).

Cross-seeding is asymmetric, and the asymmetry sits in the seeding data

Tau and α-synuclein pathology co-occurred more often in the PD group than in the AD group. One point deserves care in how it is stated. The Braak means alone do not carry the asymmetry: secondary pathology is modestly elevated above control in both disease groups — PD reaches a mean NFT stage of 2.1 against 1.4 in controls, and AD reaches a mean Lewy body stage of 1.3 against 0.4. The claim of asymmetry rests on the seeding assay and on the co-occurrence counts within individual cases, not on the group stage means, and the text should say so explicitly rather than let Figure 2 appear to do work it cannot do.

Read that way, the result is informative. α-Synuclein strains differ in their capacity to template tau, and at least one does so efficiently in neurons (Guo et al., 2013); a directional bias in which α-synuclein recruits tau more readily than the reverse would produce exactly the pattern observed. It would also help explain why so many PD patients accumulate neocortical tau as they progress to dementia, and why that co-pathology predicts cognitive decline better than Lewy pathology alone (Irwin et al., 2013). The strain framework supplies the mechanism: if conformation determines both regional pattern and rate (Kaufman et al., 2016), it may equally determine which heterologous protein a given assembly can recruit.

Three limitations bound the conclusions. The transgenic models overexpress mutant protein, so rates here are not rates in sporadic disease. The human data are cross-sectional, and a stage-correlated measure is not a demonstration of movement within one brain. And co-occurrence in tissue does not by itself establish that one protein seeded the other in that patient — shared upstream drivers remain possible. The convergence across the three designs is what carries the argument, not any one of them.

Conclusion

Tau and α-synuclein aggregation is template-directed and dose-dependent; transfer between neurons requires the connection between them; pathology in vivo follows the connectome rather than spatial proximity and requires an endogenous substrate; and in human brain seed-competent material scales with Braak stage, tracks histopathology, and crosses between the two proteins more often in PD than in AD. Three designs with non-overlapping weaknesses give the same answer.

The practical consequence is that the therapeutic target is the propagating species rather than the end-stage lesion, and that a biomarker reading seeding activity should move earlier than one reading deposition. The consequence for disease classification is less comfortable. If one conformer can recruit the other, the boundary between AD and PD is a description of which protein dominates in a given patient, not of two separate mechanisms — and trials that enrol by clinical diagnosis while targeting a single protein may be stratifying on the wrong variable.

REFERENCES

Every entry below was checked against the publisher or indexing record rather than cited from memory.

Braak H, Braak E. Neuropathological stageing of Alzheimer-related changes. *Acta Neuropathologica.* 1991;82(4):239–259.

Braak H, Del Tredici K, Rüb U, de Vos RAI, Jansen Steur ENH, Braak E. Staging of brain pathology related to sporadic Parkinson's disease. *Neurobiology of Aging.* 2003;24(2):197–211.

Clavaguera F, Bolmont T, Crowther RA, Abramowski D, Frank S, Probst A, Fraser G, Stalder AK, Beibel M, Staufenbiel M, Jucker M, Goedert M, Tolnay M. Transmission and spreading of tauopathy in transgenic mouse brain. *Nature Cell Biology.* 2009;11(7):909–913.

de Calignon A, Polydoro M, Suárez-Calvet M, William C, Adamowicz DH, Kopeikina KJ, Pitstick R, Sahara N, Ashe KH, Carlson GA, Spires-Jones TL, Hyman BT. Propagation of tau pathology in a model of early Alzheimer's disease. *Neuron.* 2012;73(4):685–697.

Guo JL, Covell DJ, Daniels JP, Iba M, Stieber A, Zhang B, Riddle DM, Kwong LK, Xu Y, Trojanowski JQ, Lee VM. Distinct α-synuclein strains differentially promote tau inclusions in neurons. *Cell.* 2013;154(1):103–117.

Holmes BB, Furman JL, Mahan TE, Yamasaki TR, Mirbaha H, Eades WC, Belaygorod L, Cairns NJ, Holtzman DM, Diamond MI. Proteopathic tau seeding predicts tauopathy in vivo. *Proceedings of the National Academy of Sciences USA.* 2014;111(41):E4376–E4385.

Irwin DJ, Lee VM, Trojanowski JQ. Parkinson's disease dementia: convergence of α-synuclein, tau and amyloid-β pathologies. *Nature Reviews Neuroscience.* 2013;14(9):626–636.

Kaufman SK, Sanders DW, Thomas TL, Ruchinskas AJ, Vaquer-Alicea J, Sharma AM, Miller TM, Diamond MI. Tau prion strains dictate patterns of cell pathology, progression rate, and regional vulnerability in vivo. *Neuron.* 2016;92(4):796–812.

Luk KC, Kehm V, Carroll J, Zhang B, O'Brien P, Trojanowski JQ, Lee VM-Y. Pathological α-synuclein transmission initiates Parkinson-like neurodegeneration in non-transgenic mice. *Science.* 2012;338(6109):949–953.

Volpicelli-Daley LA, Luk KC, Patel TP, Tanik SA, Riddle DM, Stieber A, Meaney DF, Trojanowski JQ, Lee VM. Exogenous α-synuclein fibrils induce Lewy body pathology leading to synaptic dysfunction and neuron death. *Neuron.* 2011;72(1):57–71.

IEER Institute for Excellence in Education & Research

Volpicelli-Daley LA, Luk KC, Lee VM. Addition of exogenous α-synuclein preformed fibrils to primary neuronal cultures to seed recruitment of endogenous α-synuclein to Lewy body and Lewy neurite-like aggregates. *Nature Protocols*. 2014;9(9):2135–2146.

IEER
Institute for Excellence in Education & Research